



LINEAR SUPERPOSITION OF CHAOTIC AND ORDERLY VIBRATIONS ON TWO SERIALLY CONNECTED STRINGS WITH A VAN DER POL JOINT

GOONG CHEN* and JIANXIN ZHOU*

*Department of Mathematics, Texas A&M University,
College Station, TX 77843, USA*

SZE-BI HSU†

*Institute of Applied Mathematics, National Tsing Hua University,
Hsinchu, Taiwan, R.O.C.*

Received July 18, 1995; Revised October 20, 1995

Two identical vibrating strings are serially coupled end-to-end with nonlinear joints that behave like a Van der Pol oscillator. This coupled PDE system has an infinite dimensional center manifold of orderly periodic solutions of vibration for which the nonlinearity at the joint is not excited. Based upon the authors' study of chaotic vibration on a single vibrating string in [Chen *et al.*, 1995], we analyze the special structure of the nonlinear reflection operator by decoupling. The decoupled operator has a linear part which is idempotent, and this linear part does not interact with the iterates of the nonlinear part. Using this, we show that chaotic vibrations and orderly periodic vibrations coexist and satisfy a certain rule of linear superposition, namely, if u is a linear periodic solution and if U is a general nonlinear solution, then $U + Cu$ is also a solution for any constant C . Numerical simulations and computer graphics are also included to illustrate the superposition effect.

1. Introduction

The study of nonlinear vibrations and oscillations is important in science and technology [Stoker, 1950]. In particular, *chaotic vibrations* in mechanical and electronic systems governed by second order nonlinear *ODEs* have become a focal area of this research, with rapid progress [Chen & Dong, 1993; Guckenheimer & Holmes, 1983; Moon, 1987; Wiggins, 1990] being witnessed during the past two decades. Since mechanical devices or electronic circuits often appear in serial and/or parallel connections, that is to say, *in coupled form*, chaos in

such coupled systems has attracted the attention of many investigators. See for example [SIAM, 1995] for a collection of the latest work in this area.

More recently, chaotic vibrations in some nonlinear system governed by *PDEs* have also been probed; see [Chen *et al.*, 1995] for the work by the authors. In [Chen *et al.*, 1995], only a single vibrating string was considered. The string itself satisfies the one-dimensional linear wave equation, but in one of the boundary conditions there is nonlinearity, causing chaos when the parameters enter a certain range.

*E-mail: gchen@math.tamu.edu and jzhou@math.tamu.edu

†E-mail: sbhsu@am.nthu.edu.tw

Here, we consider the situation of two serially connected linear vibrating strings, but with a non-linear coupling at the linkage. We wish to investigate chaotic phenomena arising from this coupled infinite-dimensional vibrating system.

The simplest form of coupling between two vibrating strings is serial connection [Chen & Zhou, 1993, pp. 40–51]. Here, for mathematical tractability, we consider two identical strings, with “Van der Pol” types of nonlinear transmission conditions at the joint. The mathematical models and motivations are described in some detail in Sec. 2.

In Sec. 3, we use the method of characteristics to transform the coupled vibrating strings into a diagonalized hyperbolic system. The solution of the hyperbolic system is completely determined by the reflection relation between incoming and outgoing waves at the two end points of the x -interval. The reflection relation is an *implicit* nonlinear 2×2 system. The key point here is that we are able to *decouple* the nonlinear 2×2 system, leading to a single nonlinear equation of the same type as studied by us in [Chen et al., 1995]. This nonlinear equation induces an *interval map*.

In Sec. 4, we use the basic theorems in [Chen et al., 1995] to study the chaotic or nonchaotic behavior of the iterates of that interval map, which determine the chaotic or nonchaotic properties of the coupled PDE system. Main theorems are proven here, showing that linear vibrations and chaotic vibrations can *coexist*, and under certain conditions linear and chaotic vibrations satisfy a certain *rule of linear superposition*. This is the major finding of the paper.

In Sec. 5, the last section, numerical simulations and computer graphics are presented to help visualization and to illustrate the theory.

2. Two Linear Vibrating Strings with Van der Pol Type Coupling Conditions at the Joint

A vibrating string modelled by the 1 - D wave equation

$$w_{tt}(x, t) - c^2 w_{xx}(x, t) = 0, \quad 0 < x < 1, \quad t > 0, \tag{2.1}$$

is certainly one of the simplest possible distributed parameter vibrating systems in existence. Under the usual fixed end or free end boundary conditions at $x = 0$ and $x = 1$, (2.1) is known to have an

infinite set of (L^2 -) orthonormal eigenmodes $\phi_k(x)$ with corresponding eigenfrequencies ω_k that satisfy

$$\phi_k''(x) + \omega_k^2 \phi_k(x) = 0, \quad k = 1, 2, \dots, \quad 0 < x < 1, \tag{2.2}$$

the equation of a simple linear harmonic oscillator. For this reason, (2.1) is also recognized as an *infinite dimensional harmonic oscillator*.

Let us consider the case of two coupled vibrating strings. They can be connected in many different configurations; see [Lagnese et al., 1994], for example. The simplest such configuration is *serial connection*. Let the vertical displacement w_1 and w_2 of the two linear vibrating strings satisfy, respectively, the wave equation

$$m_1 w_{1tt}(x, t) - T_1 w_{1xx}(x, t) = 0, \tag{2.3}$$

$$-1 < x < 0, \quad t > 0,$$

$$m_2 w_{2tt}(x, t) - T_2 w_{2xx}(x, t) = 0, \tag{2.4}$$

$$0 < x < 1, \quad t > 0,$$

where $m_i > 0$ and $T_i > 0$, $i = 1, 2$, are, respectively, the mass density per unit length and tension on the i th string. At the middle point $x = 0$, the two strings are coupled. It is known [Chen & Zhou, 1993, pp. 40–51] that for serial connection only two types of coupling or transmission conditions are possible pragmatically:

(Type I) Continuity of displacement, discontinuity of force:

$$\left. \begin{aligned} w_1(0, t) &= w_2(0, t), \\ T_1 w_{1x}(0, t) - T_2 w_{2x}(0, t) &= f(t), \end{aligned} \right\} \quad t > 0; \tag{2.5}$$

(Type II) Continuity of force, discontinuity of velocity (and displacement)

$$\left. \begin{aligned} T_1 w_{1x}(0, t) &= T_2 w_{2x}(0, t), \\ w_{1t}(0, t) - w_{2t}(0, t) &= g(t), \end{aligned} \right\} \quad t > 0, \tag{2.6}$$

where $f(t)$ and $g(t)$ in (2.5) and (2.6) are certain functions which are often prescribed in “*feedback form*”. For example, let us choose a *velocity feedback*

$$f(t) = -\gamma_1 w_{1t}(0, t) (= -\gamma_1 w_{2t}(0, t)), \quad \gamma_1 > 0, \tag{2.7}$$

in (2.5) for Type I coupling. Assume that strings 1 and 2 are, respectively, fixed at the left end and right end:

$$w_1(-1, t) = 0, \quad w_2(1, t) = 0, \quad t > 0. \tag{2.8}$$

The total energy of the coupled string system at time t is given by

$$E(t) = \frac{1}{2} \left\{ \int_{-1}^0 [m_1 w_{1t}^2(x, t) + T_1 w_{1x}^2(x, t)] dx + \int_0^1 [m_2 w_{2t}^2(x, t) + T_2 w_{2x}^2(x, t)] dx \right\}. \tag{2.9}$$

The rate of change of energy is found to satisfy

$$\begin{aligned} \frac{d}{dt} E(t) &= \int_{-1}^0 [m_1 w_{1t} w_{1tt} + T_1 w_{1x} w_{1xt}] dx \\ &\quad + \int_0^1 [m_2 w_{2t} w_{2tt} + T_2 w_{2x} w_{2xt}] dx \\ &\Rightarrow \text{(integrating by parts and utilizing} \\ &\quad \text{(2.3)-(2.5), (2.7), (2.8))} \Rightarrow \\ &= -\gamma_1 w_{1t}^2(0, t) \leq 0, \end{aligned} \tag{2.10}$$

and therefore energy is *nonincreasing*.

Similarly, if in (2.6), we choose a *force feedback*

$$g(t) = -\gamma_2 T_1 W_{1x}(0, t) (= -\gamma_2 T_2 w_{2x}(0, t)), \quad \gamma > 0, \tag{2.11}$$

then for this Type II joint,

$$\frac{d}{dt} E(t) = -\gamma_2 [T_1 w_{1x}(0, t)]^2 \leq 0, \tag{2.12}$$

and again the energy is *nonincreasing*. The choices of feedback (2.7) and (2.11) make the coupled system *dissipative* and thus have a *stabilizing effect* on vibration; their mechanical designs are depicted in [Chen & Zhou, 1993, pp. 50–51]. We include them here for the convenience of the readers; see Figs. 1 and 2.

Now, instead of the linear feedbacks (2.7) and (2.11), we consider *nonlinear feedbacks of Van der Pol type*. We let (2.7) be replaced by

$$f(t) = \alpha_I w_{1t}(0, t) - \beta_I w_{1t}^3(0, t); \quad \alpha_I, \beta_I > 0, \tag{2.13}$$

while all the other conditions remain unchanged. Then (2.10) is replaced by

$$\begin{aligned} \frac{d}{dt} E(t) &= \alpha_I w_{1t}^2(0, t) - \beta_I w_{1t}^4(0, t) \\ &\times \begin{cases} \leq 0 & \text{if } |w_{1t}(0, t)| \geq \left(\frac{\alpha_I}{\beta_I}\right)^{1/2}, \\ > 0 & \text{if } |w_{1t}(0, t)| < \left(\frac{\alpha_I}{\beta_I}\right)^{1/2}. \end{cases} \end{aligned} \tag{2.14}$$

Therefore, similarly to the case of a single string [Chen *et al.*, 1995], we see that the coupling conditions (2.5) + (2.13) have a *self-regulating* effect: if the total energy is increasing, then the magnitude of velocity at the joint will become small, and conversely, if the total energy is decreasing, then the magnitude of velocity at the joint will become large. Analogously, if we replace (2.11) by

$$g(t) = \alpha_{II} [T_1 w_{1x}(0, t)] - \beta_{II} [T_1 w_{1x}(0, t)]^2; \quad \alpha_{II}, \beta_{II} > 0, \tag{2.15}$$

then in lieu of (2.12) we have

$$\begin{aligned} \frac{d}{dt} E(t) &= \alpha_{II} [T_1 w_{1x}(0, t)]^2 - \beta_{II} [T_1 w_{1x}(0, t)]^4 \\ &\times \begin{cases} \leq 0 & \text{if } |T_1 w_{1x}(0, t)| \geq \left(\frac{\alpha_{II}}{\beta_{II}}\right)^{1/2}, \\ > 0 & \text{if } |T_1 w_{1x}(0, t)| < \left(\frac{\alpha_{II}}{\beta_{II}}\right)^{1/2}. \end{cases} \end{aligned} \tag{2.16}$$

From (2.14) and (2.16), obviously, we see that the coupled string system will have bounded energy for all time $t > 0$. But *will the nonlinear coupling conditions cause chaos?* This is the major subject we are interested to explore here.

The method to be employed by us in the next section will be the *method of characteristics*. For mathematical tractability, we assume that the two strings (2.3) and (2.4) are identical: $m_1 = m_2$ and $T_1 = T_2$. Since the wave speed $c_i = (T_i/m_i)^{1/2}$ plays only a very minor role in the ensuing analysis, we simply set $m_1 = m_2 = 1$ and $T_1 = T_2 = 1$. (The assumption that $c_1 = c_2$ will *not be robust* as far as our later theorems are concerned. We nevertheless hope that this study will motivate others to derive more robust results in the future.) For the ease and clarity of future reference, we re-list the system of equations under study here:

$$\text{(PDEs)} \quad \begin{cases} w_{1tt}(x, t) - w_{1xx}(x, t) = 0, \\ \quad -1 < x < 0, \quad t > 0, \\ w_{2tt}(x, t) - w_{2xx}(x, t) = 0, \\ \quad 0 < x < 1, \quad t > 0; \end{cases} \tag{2.17}$$

$$\begin{aligned} \text{(left end boundary} & \quad w_1(-1, t) = 0, \quad t > 0, \\ \text{condition)} & \end{aligned} \tag{2.18}$$

$$\begin{aligned} \text{(right end boundary} & \quad w_2(1, t) = 0, \quad t > 0; \\ \text{condition)} & \end{aligned} \tag{2.19}$$

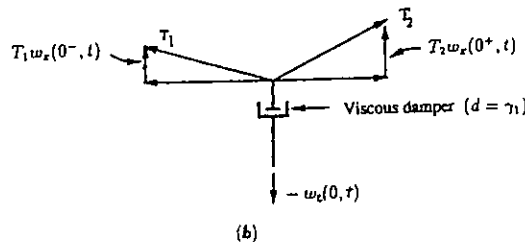
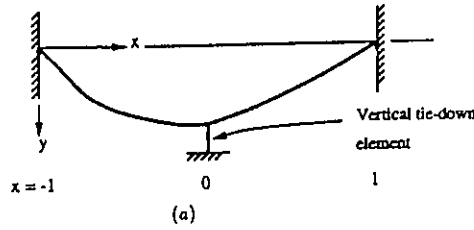
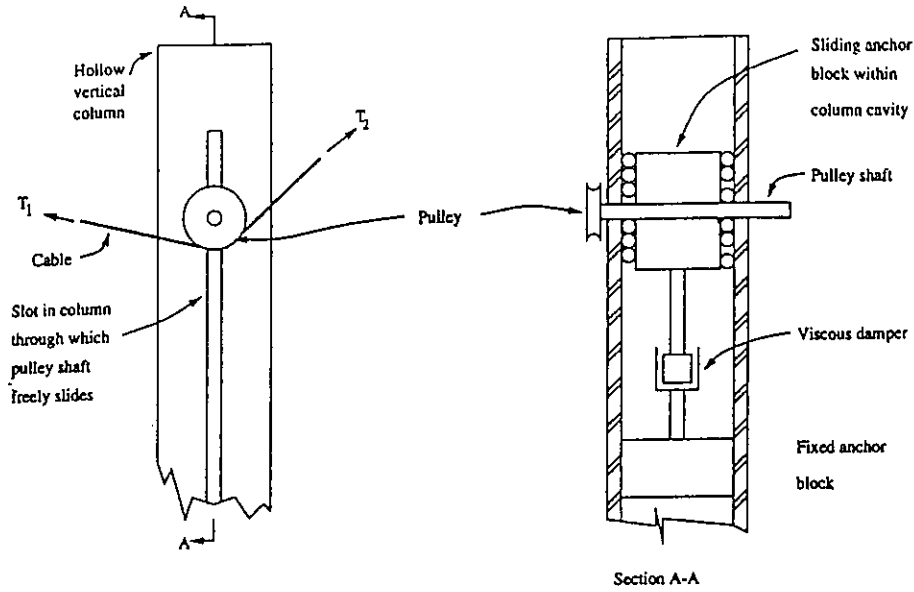


Fig. 1. Mechanical design and structural analysis of a dissipative joint satisfying the transmission conditions (2.5) and (2.7), where displacement is continuous across the joint, but the tension force is discontinuous with velocity feedback. (Reprinted from [Chen & Zhou, 1993], courtesy of CRC Press, Boca Raton, Florida.)

(Van der Pol joint, Type I):

$$\begin{cases} w_1(0, t) = w_2(0, t), \\ w_{1x}(0, t) - w_{2x}(0, t) = \alpha_I w_{1t}(0, t) - \beta_I w_{1t}^3(0, t); \quad \alpha_I, \beta_I > 0; \end{cases} \quad (2.20)$$

(Van der Pol joint, Type II):

$$\begin{cases} w_{1x}(0, t) = w_{2x}(0, t), \\ w_{1t}(0, t) - w_{2t}(0, t) = \alpha_{II} w_{1x}(0, t) - \beta_{II} w_{1x}^3(0, t); \quad \alpha_{II}, \beta_{II} > 0. \end{cases} \quad (2.21)$$

(initial conditions):

$$\begin{cases} w_1(x, 0) = w_{1,0}(x) \in C^1([-1, 0]), & w_{1t}(x, 0) = v_{1,0}(x) \in C^0([-1, 0]), \\ w_2(x, 0) = w_{2,0}(x) \in C^1([0, 1]), & w_{2t}(x, 0) = v_{2,0}(x) \in C^0([0, 1]); \end{cases} \quad (2.22)$$

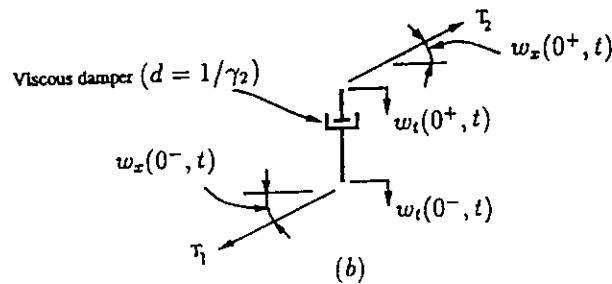
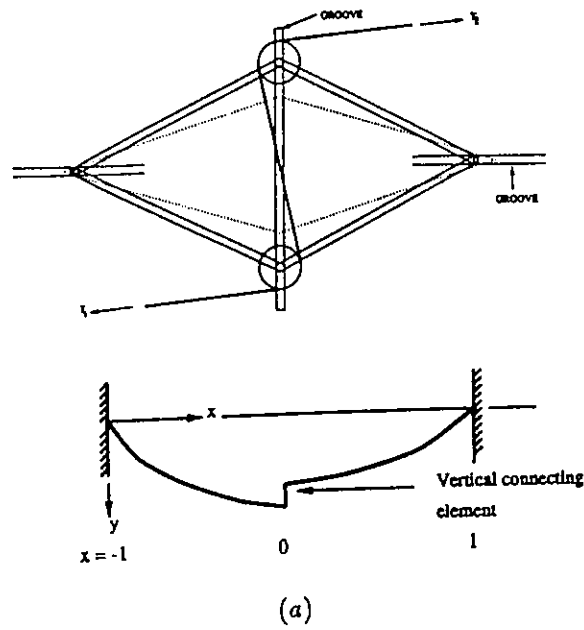
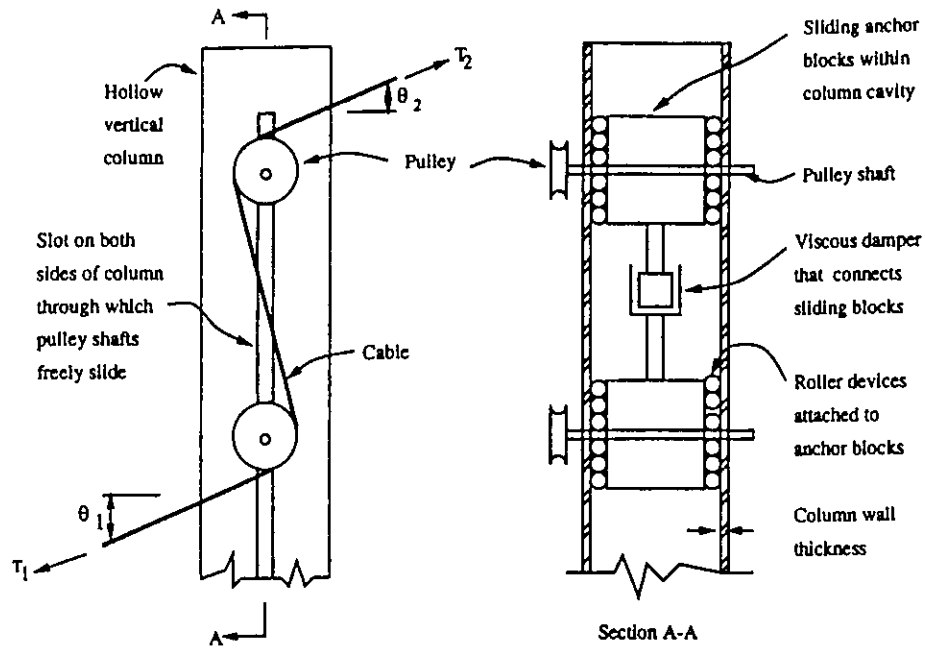


Fig. 2. Mechanical design and structural analysis of a dissipative joint satisfying the transmission conditions (2.6) and (2.11), where the tension force is continuous across the joint, but the displacement is discontinuous with tension force feedback. (Reprinted from [Chen & Zhou, 1993], courtesy of CRC Press, Boca Raton, Florida.)

Before passing, let us point out some useful observation. Consider (2.17)–(2.20). Despite the nonlinearity in (2.20), this system contains infinitely many eigenmodes or eigensolutions of the form

$$\left. \begin{matrix} w_{1,n}(x, t) \\ w_{2,n}(x, t) \end{matrix} \right\} = (c_{1n} \cos n\pi t + c_{2n} \sin n\pi t) \sin n\pi x, \begin{cases} -1 \leq x \leq 0, \\ 0 \leq x \leq 1, \end{cases} \quad (2.23)$$

for $c_{1n}, c_{2n} \in \mathbb{R}, n = 1, 2, 3, \dots$, s.t. their linear superposition

$$\left. \begin{matrix} w_1(x, t) \\ w_2(x, t) \end{matrix} \right\} = \sum_{n=1}^{\infty} (c_{1n} \cos n\pi t + c_{2n} \sin n\pi t) \sin n\pi x, \begin{cases} -1 \leq x \leq 0, \\ 0 \leq x \leq 1, \end{cases} \quad (2.24)$$

is again a solution of (2.17)–(2.20) (provided that the coefficients c_{1n} and $c_{2n}, n = 1, 2, \dots$, taper off to zero sufficiently fast.) The reason is that the midpoint $x = 0$ happens to be a *nodal point* of the eigenmode (2.23), therefore

$$\frac{\partial}{\partial t} w_{1,n}(0, t) = \frac{\partial}{\partial t} w_{2,n}(0, t) = 0, \quad t > 0,$$

and the *nonlinearity is not excited* so the RHS of the second equation in (2.21) is zero for all $t > 0$.

Similarly, for (2.17)–(2.19) and (2.21), this system has infinitely many eigensolutions of the form

$$\left. \begin{matrix} w_{1n}(x, t) \\ w_{2n}(x, t) \end{matrix} \right\} = \left[d_{1n} \cos \left(n + \frac{1}{2} \right) \pi t + d_{2n} \sin \left(n + \frac{1}{2} \right) \pi t \right] \cos \left(n + \frac{1}{2} \right) \pi x, \begin{cases} -1 \leq x \leq 0, \\ 0 \leq x \leq 1, \end{cases} \quad (2.25)$$

for $d_{1n}, d_{2n} \in \mathbb{R}, n = 0, 1, 2, \dots$ s.t. their superposition

$$\left. \begin{matrix} w_1(x, t) \\ w_2(x, t) \end{matrix} \right\} = \sum_{n=0}^{\infty} \left[d_{1n} \cos \left(n + \frac{1}{2} \right) \pi t + d_{2n} \sin \left(n + \frac{1}{2} \right) \pi t \right] \cos \left(n + \frac{1}{2} \right) \pi x, \begin{cases} -1 \leq x \leq 0, \\ 0 \leq x \leq 1. \end{cases} \quad (2.26)$$

is again a solution of (2.17)–(2.19) and (2.21), because $x = 0$ is also a “nodal point” of the eigen-solution (2.25) in the sense that the nonlinearity in (2.21) is not excited at $x = 0$.

In summary, the system (2.17)–(2.22) with a Van der Pol joint of either Type I or Type II admits an infinite dimensional solution submanifold which forms a vector space. Such solutions in this linear submanifold are said to constitute *orderly vibrations* of the problem under study.

3. A 2×2 System of Nonlinear Reflection Relation and Its Decoupling

We use the method of characteristics to convert (2.17) into a diagonalized first order hyperbolic system. For $x : 0 < x < 1$ and $t > 0$, define

$$\begin{aligned} u_1(x, t) &= \frac{1}{2} \left[\frac{\partial}{\partial x} w_1(-x, t) + \frac{\partial}{\partial t} w_1(-x, t) \right] \\ &= \frac{1}{2} [-w_{1x}(-x, t) + w_{1t}(-x, t)]. \end{aligned} \quad (3.1)$$

Then

$$\begin{aligned} \frac{\partial}{\partial t} u_1(x, t) &= \frac{1}{2} [-w_{1xt}(-x, t) + w_{1tt}(-x, t)] \\ &= \frac{1}{2} [-w_{1xt}(-x, t) + w_{1xx}(-x, t)] \\ &= \frac{\partial}{\partial x} \left\{ \frac{1}{2} [-w_{1x}(-x, t) + w_{1t}(-x, t)] \right\} \\ &= \frac{\partial}{\partial x} u_1(x, t). \end{aligned}$$

Similarly, define

$$v_1(x, t) = -\frac{1}{2} [w_{1x}(-x, t) + w_{1t}(-x, t)], \quad (3.2)$$

$$u_2(x, t) = \frac{1}{2} [w_{2x}(x, t) + w_{2t}(x, t)], \quad (3.3)$$

$$v_2(x, t) = \frac{1}{2} [w_{2x}(x, t) - w_{2t}(x, t)]. \quad (3.4)$$

Then we obtain

$$\frac{\partial}{\partial t} \begin{bmatrix} u_1(x, t) \\ v_1(x, t) \\ u_2(x, t) \\ v_2(x, t) \end{bmatrix} = \begin{bmatrix} 1 & 0 & 0 & 0 \\ 0 & -1 & 0 & 0 \\ 0 & 0 & 1 & 0 \\ 0 & 0 & 0 & -1 \end{bmatrix} \frac{\partial}{\partial x} \begin{bmatrix} u_1(x, t) \\ v_1(x, t) \\ u_2(x, t) \\ v_2(x, t) \end{bmatrix}, \quad 0 < x < 1, \quad t > 0. \quad (3.5)$$

The relationships between u_1, v_1, u_2 and v_2 and the gradient of w_1 and w_2 are

$$\left. \begin{aligned} w_{1x}(x, t) &= -[u_1(-x, t) + v_1(-x, t)], \\ w_{1t}(x, t) &= u_1(-x, t) - v_1(-x, t), \end{aligned} \right\} -1 < x < 0, \quad t > 0, \quad (3.6)$$

$$\left. \begin{aligned} w_{2x}(x, t) &= u_2(x, t) + v_2(x, t), \\ w_{2t}(x, t) &= u_2(x, t) - v_2(x, t), \end{aligned} \right\} 0 < x < 1, \quad t > 0. \quad (3.7)$$

The boundary and transmission conditions (2.18)–(2.21) have been transformed into the following: At $x = 1$:

$$u_1(1, t) = v_1(1, t), \quad (\text{from (2.18) and (3.6)}) \quad (3.8)$$

$$u_2(1, t) = v_2(1, t); \quad (\text{from (2.19) and (3.7)}) \quad (3.9)$$

at $x = 0$:

$$\text{(Type I joint)} \left\{ \begin{aligned} \beta_I(v_1 - u_1)^3 - \alpha_I(v_1 - u_1) + (u_1 + v_1) + (u_2 + v_2) &= 0, \\ v_1 - u_1 &= v_2 - u_2, \end{aligned} \right\} t > 0; \quad (3.10)$$

$$\text{(Type II joint)} \left\{ \begin{aligned} \beta_{II}(v_1 + u_1)^3 - \alpha_{II}(v_1 + u_1) + (v_1 - u_1) - (v_2 - u_2) &= 0, \\ -(u_1 + v_1) &= u_2 + v_2, \end{aligned} \right\} t > 0. \quad (3.11)$$

The components $v_1(x, t)$ and $v_2(x, t)$ are constant along the characteristics $x - t = \text{constant}$. Once these characteristics hit the right boundary $x = 1$, a reflection is made according to (3.8) and (3.9). Similarly, the components $u_1(x, t)$ and $u_2(x, t)$ are constant along the characteristics $x + t = \text{constant}$. Once these characteristics hit the left boundary $x = 0$, a reflection is made according to (3.10) or (3.11), depending on which type of joint is installed at $x = 0$. Here we need to solve $v_1(0, t)$ and $v_2(0, t)$ in terms of $u_1(0, t)$ and $u_2(0, t)$ by (3.10) or (3.11) using Cardan’s formula for cubic algebraic equations. But, as pointed out in [Chen *et al.*, 1995, Sec. 2], given u_1 and u_2 , (real) solutions v_1 and v_2 for (3.10) or (3.11) will *not be unique* for a range of the parameter α_I or α_{II} . This implies that weak solutions to the PDE system (3.5), (3.8)–(3.11), plus initial conditions, will not be unique in general. This nonuniqueness issue will be resolved shortly. Assume for now that with given values of $\alpha_I, \beta_I, \alpha_{II}, \beta_{II} > 0$ in (3.10) and (3.11), we can choose a unique pair of (v_1, v_2) from (u_1, u_2) such that (3.10) or (3.11) is satisfied. We write this dependence as

$$\begin{bmatrix} v_1 \\ v_2 \end{bmatrix} = \mathcal{F} \left(\begin{bmatrix} u_1 \\ u_2 \end{bmatrix} \right) = \begin{bmatrix} \mathcal{F}_1(u_1, u_2) \\ \mathcal{F}_2(u_1, u_2) \end{bmatrix}. \quad (3.12)$$

Then the solution $(u_1(x, t), v_1(x, t), u_2(x, t), v_2(x, t))$ is unique (according to (3.12)) and is given by the following: for $(x, t), 0 \leq x \leq 1, t = 2k + \tau, k = 0, 1, 2, \dots, 0 \leq \tau < 2,$

$$\begin{bmatrix} v_1(x, t) \\ v_2(x, t) \end{bmatrix} = \begin{cases} \mathcal{F}^k \left(\begin{bmatrix} v_{1,0}(x - \tau) \\ v_{2,0}(x - \tau) \end{bmatrix} \right), & \tau \leq x, \\ \mathcal{F}^{k+1} \left(\begin{bmatrix} u_{1,0}(\tau - x) \\ u_{2,0}(\tau - x) \end{bmatrix} \right), & x < \tau \leq 1 + x, \\ \mathcal{F}^{k+1} \left(\begin{bmatrix} v_{1,0}(2 - \tau + x) \\ v_{2,0}(2 - \tau + x) \end{bmatrix} \right), & 1 + x < \tau \leq 2, \end{cases} \quad (3.13)$$

$$\begin{bmatrix} u_1(x, t) \\ u_2(x, t) \end{bmatrix} = \begin{cases} \mathcal{F}^k \left(\begin{bmatrix} u_{1,0}(x + \tau) \\ u_{2,0}(x + \tau) \end{bmatrix} \right), & x + \tau \leq 1, \\ \mathcal{F}^k \left(\begin{bmatrix} v_{1,0}(2 - x - \tau) \\ v_{2,0}(2 - x - \tau) \end{bmatrix} \right), & 1 < x + \tau \leq 2, \\ \mathcal{F}^{k+1} \left(\begin{bmatrix} u_{1,0}(x + \tau - 2) \\ u_{2,0}(x + \tau - 2) \end{bmatrix} \right), & 2 < x + \tau, \end{cases} \tag{3.14}$$

where $v_{1,0}, v_{2,0}, u_{1,0}$ and $u_{2,0}$ are the initial conditions for v_1, v_2, u_1 and u_2 , respectively. From the above formulas, obviously chaos occurs if the iterates \mathcal{F}^n of mapping (3.12) is “chaotic” in a certain sense. Therefore \mathcal{F} is the natural “Poincaré map” for the PDE system.

The determination of chaotic behavior for (3.12) is harder than the case of a single scalar interval map studied in [Chen et al., 1995] because (3.2) is a 2×2 nonlinear system. Fortunately, we have found that the study of (3.12) is reducible to a single scalar implicit cubic equation of the same type in [Chen et al., 1995] through *decoupling*. This procedure is described below:

Decoupling for Type I joint:

From (3.10), define

$$V_I = v_1 + v_2, \quad U_I = u_1 + u_2. \tag{3.15}$$

Then from the second equation in (3.10), the first of (3.10) can be rewritten as

$$\begin{aligned} & \beta_I \left\{ \frac{1}{2} [(v_1 - u_1) + (v_2 - u_2)] \right\}^3 \\ & - \alpha_I \left\{ \frac{1}{2} [(v_1 - u_1) + (v_2 - u_2)] \right\} \\ & + [(v_1 - u_1) + (v_2 - u_2)] + 2(u_1 + u_2) = 0, \end{aligned}$$

or

$$\frac{\beta_I}{8} (V_I - U_I)^3 + \left(1 - \frac{\alpha_I}{2} \right) (V_I - U_I) + 2U_I = 0. \tag{3.16}$$

Decoupling for Type II joint:

From (3.11), define

$$V_{II} = v_1 - v_2, \quad U_{II} = -(u_1 - u_2). \tag{3.17}$$

Then the first equation of (3.11) can be rewritten as

$$\begin{aligned} & \beta_{II} \left\{ \frac{1}{2} [(v_1 + u_1) - (v_2 + u_2)] \right\}^3 \\ & - \alpha_{II} \left\{ \frac{1}{2} [(v_1 + u_1) - (v_2 + u_2)] \right\} \\ & + [(v_1 + u_1) - (v_2 + u_2)] - 2(u_1 + u_2) = 0, \end{aligned}$$

or

$$\frac{\beta_{II}}{8} (V_{II} - U_{II})^3 + \left(1 - \frac{\alpha_{II}}{2} \right) (V_{II} - U_{II}) + 2U_{II} = 0, \tag{3.18}$$

the form of which is identical to (3.16).

Note that both (3.16) and (3.18), except for the notation of coefficients α_i, β_i and the variables $U_i, V_i, i = I, II$, are identical in form to the equation

$$\beta(u - v)^3 + (1 - \alpha)(u - v) + 2v = 0; \quad \alpha, \beta > 0, \tag{3.19}$$

studied in [Chen et al., 1995, (3.1)]. To make this paper sufficiently self-contained, let us recapitulate the relevant information from [Chen et al., 1995] below.

From Cardan’s formula (see the discussion in [Chen et al., 1995, Sec. 2]), we know that for (3.19),

- (i) if $0 < \alpha \leq 1, \beta > 0$, then for each given $v \in \mathbb{R}$, there exists a unique real solution $u \in \mathbb{R}$ satisfying (3.19). This defines a single-valued mapping $u = F(v)$.
- (ii) if $\alpha > 1, \beta > 0$, then for each given $v \in \mathbb{R}$, there exist multiple solutions $u \in \mathbb{R}$ satisfying (3.19):

- (a) if $|v| > v^* \equiv \frac{\alpha-1}{3} \sqrt{\frac{\alpha-1}{3\beta}}$, then there exists a unique $u \in \mathbb{R}$ satisfying (3.19), with

$$\begin{aligned} u = v + & \left\{ -\frac{v}{\beta} + \left[\frac{(1 - \alpha)^3}{27\beta^3} + \frac{v^2}{\beta^2} \right]^{\frac{1}{2}} \right\}^{\frac{1}{3}} \\ & + \left\{ -\frac{v}{\beta} - \left[\frac{(1 - \alpha)^3}{27\beta^3} + \frac{v^2}{\beta^2} \right]^{\frac{1}{2}} \right\}^{\frac{1}{3}}; \end{aligned} \tag{3.20}$$

- (b) if $|v| < v^*$, then there exist three distinct

real $u_i \in \mathbb{R}$, $i = 1, 2, 3$, satisfying (3.19):

$$u_1 = v + \left\{ -\frac{v}{\beta} + \left[\frac{(1-\alpha)^3}{27\beta^3} + \frac{v^2}{\beta^2} \right]^{\frac{1}{2}} \right\}^{\frac{1}{3}} + \left\{ -\frac{v}{\beta} - \left[\frac{(1-\alpha)^3}{27\beta^3} + \frac{v^2}{\beta^2} \right]^{\frac{1}{2}} \right\}^{\frac{1}{3}}, \tag{3.21}$$

$$u_2 = v + \omega \left\{ -\frac{v}{\beta} + \left[\frac{(1-\alpha)^3}{27\beta^3} + \frac{v^2}{\beta^2} \right]^{\frac{1}{2}} \right\}^{\frac{1}{3}} + \bar{\omega} \left\{ -\frac{v}{\beta} - \left[\frac{(1-\alpha)^3}{27\beta^3} + \frac{v^2}{\beta^2} \right]^{\frac{1}{2}} \right\}^{\frac{1}{3}}, \tag{3.22}$$

$$u_3 = v + \bar{\omega} \left\{ -\frac{v}{\beta} + \left[\frac{(1-\alpha)^3}{27\beta^3} + \frac{v^2}{\beta^2} \right]^{\frac{1}{2}} \right\}^{\frac{1}{3}} + \omega \left\{ -\frac{v}{\beta} - \left[\frac{(1-\alpha)^3}{27\beta^3} + \frac{v^2}{\beta^2} \right]^{\frac{1}{2}} \right\}^{\frac{1}{3}}; \tag{3.23}$$

$$\omega \equiv \frac{1}{2}(-1 + \sqrt{3}i), \quad \bar{\omega} \equiv \frac{1}{2}(-1 - \sqrt{3}i).$$

(c) if $|v| = v^*$, then there exist two distinct real $\tilde{u}_i \in \mathbb{R}$, $i = 1, 2$, satisfying (3.19). We may take

$$\tilde{u}_1 = \lim_{v \rightarrow v^*} \text{RHS of (3.22)},$$

$$\tilde{u}_2 = \lim_{v \rightarrow -v^*} \text{RHS of (3.23)}.$$

The convention to choose a single-valued function $u = F(v)$ in [Chen *et al.*, 1995] is made as follows:

$$u = F(v) = \begin{cases} \text{RHS of (3.20)}, & \text{if } |v| > v^*, \\ \text{RHS of (3.21)}, & \text{if } |v| < v^*, \\ \text{limit of RHS of (3.20)}, & \text{if } v = \pm v^*. \end{cases} \tag{3.24}$$

In either (i) or (ii), the mapping $F : \mathbb{R} \rightarrow \mathbb{R}$ will have a global (not necessarily minimal) invariant rectangle $\mathcal{I} \equiv I \times I \subseteq \mathbb{R}^2$ in the phase plane, where I is a closed connected interval in \mathbb{R} , s.t. $F : I \rightarrow I$.

In case (i), F has a unique repelling fixed point $0 : 0 = F(0)$; all the other points are attracted

to a unique pair of attracting period-2 fixed points $\pm v_{p2} : -v_{p2} = F(v_{p2})$, $v_{p2} = F(-v_{p2})$. Therefore the map F is not chaotic as an interval map.

In case (ii), the interval $I \equiv [-a, a]$ contains $\pm v^*$ in the interior of I . Let A be a closed subinterval of I . Following Keener [1980], we define a *rotation number* ρ_A (with respect to the interval A) as in [Chen *et al.*, 1995 (A.2)]: For any $x \in I$,

$$\rho_A(x) = \lim_{n \rightarrow \infty} \frac{1}{n} \sum_{k=1}^n \chi_A(F^k(x)), \quad x \in I, \tag{3.25}$$

where χ_A is the characteristic function of set A , and F^n is the n th iterate of the function F . We say that $F : I \rightarrow I$ is *chaotic* if

$$\begin{aligned} \text{range } \rho_A(x) &\supseteq (\delta_1, \delta_2), \\ &x \in I \\ 0 &\leq \delta_1 < \delta_2, \text{ for some } \delta_1, \delta_2, \end{aligned} \tag{3.26}$$

i.e., range ρ_A contains an interval (δ_1, δ_2) . Since a rational rotation number $\rho_A(x)$ corresponds to asymptotically periodic orbits, and an irrational rotation number $\rho_A(x)$ corresponds to aperiodic trajectories, the iterates $\{F^n(x) | x \in I\}$ on I are therefore rich in both periodic and aperiodic solutions, each set of which is dense in A . It has been proven in [Chen *et al.*, 1995, Sec. 4] that

$$\begin{aligned} \text{if } 3.74339\dots < \alpha < 28.27305\dots, \\ \beta > 0, \text{ then } F \text{ is chaotic.} \end{aligned} \tag{3.27}$$

Return to (3.16) and (3.18). We now adopt the convention analogous to (3.24) for (3.16) and (3.18). By comparing (3.16) and (3.18) with (3.19), and from the way $v^* = \frac{\alpha-1}{3} \sqrt{\frac{\alpha-1}{3\beta}}$ is given, we define

$$\begin{aligned} U_i^* &= \frac{\left(\frac{\alpha_i}{2} - 1\right)}{3} \sqrt{\frac{(\alpha_i/2) - 1}{3(\beta_i/8)}} \\ &= \frac{\alpha_i - 2}{3} \sqrt{\frac{\alpha_i - 2}{3\beta_i}}, \\ &i = I \text{ or } II. \end{aligned} \tag{3.28}$$

We now know that if $\alpha_i : 0 < \alpha_i \leq 2$, $\beta_i > 0$, $i = I, II$, for each given U_i , there corresponds exactly one V_i satisfying (3.16) or (3.18). This correspondence gives the single-valued function $V_i \equiv \tilde{F}(U_i)$, $i = I, II$.

But if $\alpha_i > 2, \beta_i > 0, i = I, II$, then we know that

(a)' if $|U_i| > U_i^*$, then (3.16) or (3.18) has only one real solution

$$V_i = U_i + 2 \left(\sqrt[3]{-\frac{U_i}{\beta_i} + \sqrt{-\frac{(\alpha_i - 2)^3}{27\beta_i^3} + \frac{U_i^2}{\beta_i^2}}} + \sqrt[3]{-\frac{U_i}{\beta_i} - \sqrt{-\frac{(\alpha_i - 2)^3}{27\beta_i^3} + \frac{U_i^2}{\beta_i^2}}} \right) \in \mathbb{R}, \tag{3.29}$$

for given $U_i \in \mathbb{R}$;

(b)' if $|U_i| < U_i^*$, three distinct real values of V_i satisfying (3.16) or (3.18) can be obtained for each given $U_i \in \mathbb{R}$:

$$V_i = U_i + 2 \left(\sqrt[3]{-\frac{U_i}{\beta_i} + \sqrt{-\frac{(\alpha_i - 2)^3}{27\beta_i^3} + \frac{U_i^2}{\beta_i^2}}} + \sqrt[3]{-\frac{U_i}{\beta_i} - \sqrt{-\frac{(\alpha_i - 2)^3}{27\beta_i^3} + \frac{U_i^2}{\beta_i^2}}} \right) \in \mathbb{R}, \tag{3.30}$$

$$V_i = U_i + 2 \left(\omega \sqrt[3]{-\frac{U_i}{\beta_i} + \sqrt{-\frac{(\alpha_i - 2)^3}{27\beta_i^3} + \frac{U_i^2}{\beta_i^2}}} + \bar{\omega} \sqrt[3]{-\frac{U_i}{\beta_i} - \sqrt{-\frac{(\alpha_i - 2)^3}{27\beta_i^3} + \frac{U_i^2}{\beta_i^2}}} \right) \in \mathbb{R}, \tag{3.31}$$

$$V_i = U_i + 2 \left(\bar{\omega} \sqrt[3]{-\frac{U_i}{\beta_i} + \sqrt{-\frac{(\alpha_i - 2)^3}{27\beta_i^3} + \frac{U_i^2}{\beta_i^2}}} + \omega \sqrt[3]{-\frac{U_i}{\beta_i} - \sqrt{-\frac{(\alpha_i - 2)^3}{27\beta_i^3} + \frac{U_i^2}{\beta_i^2}}} \right) \in \mathbb{R}, \tag{3.32}$$

(c)' if $U_i = \pm U_i^*$, then two distinct real values of V_i satisfying (3.16) or (3.18) can be obtained:

$$V_i = \lim_{U_i \rightarrow U_i^*} \text{RHS of (3.31)},$$

$$V_i = \lim_{U_i \rightarrow -U_i^*} \text{RHS of (3.32)}.$$

The above multi-valued correspondence (a), (b), (c) can be seen in Fig. 3(a).

We now define a single-valued function \tilde{F} by adopting the convention analogous to (3.24) for (3.16) and (3.18):

$$V_i = \tilde{F}(U_i) = \begin{cases} \text{RHS of (3.29)}, & \text{if } |U_i| > U_i^*, \\ \text{RHS of (3.30)}, & \text{if } |U_i| < U_i^*, \\ \text{limit of RHS of (3.29)}, & \text{if } U_i = \pm U_i^*, \end{cases} \tag{3.33}$$

Then this reflection relation \tilde{F} is single-valued, allowing a unique solution(s) of (2.17)–(2.22) to exist. It has the same advantages such as being skew-symmetric and mathematically tractable as in [Chen et al., 1995]. However, the relation (3.26) is not “naturally occurring” in the sense that it is not a relaxation oscillation; it can only be enforced through some control devices such as a design suggested in [Chen et al., 1995, Appendix B], for example. We again call \tilde{F} the *controlled hysterectic reflection relation*. See Fig. 3(b).

Once $V_I = v_1 + v_2$ or $V_{II} = v_1 - v_2$ has been determined respectively from \tilde{F} , then we can solve v_1 and v_2 from (3.10) and (3.11):

$$\text{(Type I joint)} \begin{cases} v_1 + v_2 = V_I = \tilde{F}(u_1 + u_2) \\ v_1 - v_2 = u_1 - u_2; \end{cases} \tag{3.34}$$

$$\text{(Type II joint)} \begin{cases} v_1 - v_2 = V_{II} = \tilde{F}(-u_1 + u_2), \\ v_1 + v_2 = -(u_1 + u_2). \end{cases} \tag{3.35}$$

This determines the relation \mathcal{F} in (3.12):

$$\begin{aligned} \text{(Type I joint)} & \begin{bmatrix} v_1 \\ v_2 \end{bmatrix} \\ &= \mathcal{F}_I \left(\begin{bmatrix} u_1 \\ u_2 \end{bmatrix} \right) \\ &\equiv \frac{1}{2} \begin{bmatrix} (u_1 - u_2) + \tilde{F}(u_1 + u_2) \\ (-u_1 + u_2) + \tilde{F}(u_1 + u_2) \end{bmatrix}; \end{aligned} \tag{3.36}$$

$$\begin{aligned} \text{(Type II joint)} & \begin{bmatrix} v_1 \\ v_2 \end{bmatrix} \\ &= \mathcal{F}_{II} \left(\begin{bmatrix} u_1 \\ u_2 \end{bmatrix} \right) \\ &\equiv \frac{1}{2} \begin{bmatrix} -(u_1 + u_2) + \tilde{F}(-u_1 + u_2) \\ -(u_1 + u_2) - \tilde{F}(-u_1 + u_2) \end{bmatrix}. \end{aligned} \tag{3.37}$$

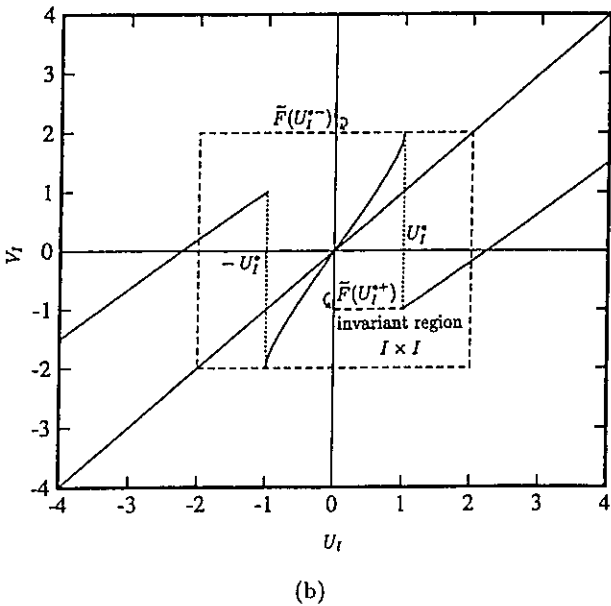
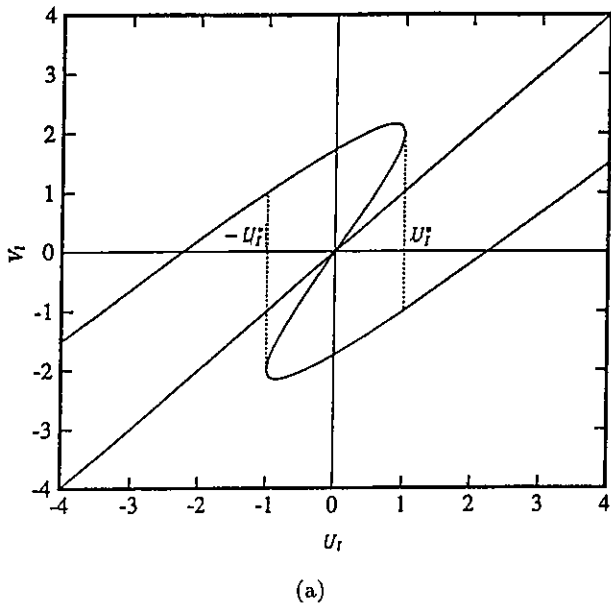


Fig. 3. (a) The multi-valued relation between U_I and V_I satisfying (3.16), with $\alpha_I = 8, \beta_I = 8$. (b) The single-valued controlled hysteretic reflection relation obtained from (a).

By using \mathcal{F}_I or \mathcal{F}_{II} in (3.13) and (3.14), the problem is solved by repeated reflections at $x = 0$ and $x = 1$ along characteristics. The 2×2 operators \mathcal{F}_I and \mathcal{F}_{II} have iterates \mathcal{F}_I^k and \mathcal{F}_{II}^k satisfying simple yet highly useful algebraic properties given below, namely, the linear part of \mathcal{F}_I or \mathcal{F}_{II} is idempotent (or odd-idempotent), and is separable from the nonlinear part.

Lemma 3.1 (Idempotency of the Linear Part and Separable Nonlinearity of \mathcal{F}_I and \mathcal{F}_{II}). We have

$$\mathcal{F}_I^k \left(\begin{bmatrix} u_1 \\ u_2 \end{bmatrix} \right) = \frac{1}{2} \left[\begin{array}{l} (u_1 - u_2) + \tilde{F}^k(u_1 + u_2) \\ (-u_1 + u_2) + \tilde{F}^k(u_1 + u_2) \end{array} \right],$$

$$\begin{aligned} \mathcal{F}_{II}^k \left(\begin{bmatrix} u_1 \\ u_2 \end{bmatrix} \right) \\ = \frac{(-1)^{k-1}}{2} \left[\begin{array}{l} -(u_1 + u_2) + (-1)^k (-\tilde{F})^k (-u_1 + u_2) \\ -(u_1 + u_2) - (-1)^k (-\tilde{F})^k (-u_1 + u_2) \end{array} \right], \end{aligned}$$

for $k = 1, 2, \dots$

Proof. The verification can be done by mathematical induction from the definitions of \mathcal{F}_I and \mathcal{F}_{II} in (3.36) and (3.37). Since the work is straightforward, we omit it here. ■

4. Linear Superposition of Chaotic and Orderly Vibrations

The solutions (3.13) and (3.14) depend on the iterates of \mathcal{F}_I or \mathcal{F}_{II} . Therefore chaotic vibrations can be associated with the chaotic properties of $\mathcal{F}_i, i = I, II$, which map \mathbb{R}^2 into \mathbb{R}^2 . Although certain methods exist for the study of dynamic behavior of multi-dimensional maps such as \mathcal{F}_i here (see for example [Devaney, 1989, Part 2], [Wiggins, 1990]), the treatment would be lengthy and tedious. Instead, we take a somewhat relaxed approach. From the representations of \mathcal{F}_I and \mathcal{F}_{II} in (3.37) and (3.37), it is obvious that chaos of \mathcal{F}_I and \mathcal{F}_{II} can only result from that of \tilde{F} , because the rest \mathcal{F}_I and \mathcal{F}_{II} involves merely linear operations. We thus define the following.

Definition 4.1. We say that $\mathcal{F}_i : \mathbb{R}^2 \rightarrow \mathbb{R}^2, i = I$ or II , is chaotic if the mapping \tilde{F} in (3.36) and (3.37) is chaotic as an interval map (satisfying (3.26)).

By (3.27), the following becomes trivial.

Theorem 4.1. If

$$7.48878 \dots < \alpha_i < 56.54610 \dots, \beta_i > 0, \quad i = I, II, \tag{4.1}$$

then \mathcal{F}_I and \mathcal{F}_{II} are chaotic.

Our limited scope of interest and emphasis in this paper is to show that for the system(s) (3.5)–(3.11), although there is the presence of nonlinearity in Van der Pol joints of Type I or Type II, both

orderly vibrations and chaotic vibrations can occur, and two such vibrations can be linearly superposed.

Our first theorem characterizes the condition of linear vibrations.

Theorem 4.2 (*Linear Solutions of Two Nonlinearly Coupled Strings with a Type I Joint*). Consider the PDE system (3.5) and (3.8)–(3.10), with $\alpha_I > 0$ and $\beta_I > 0$ in (3.10) and with given initial conditions $u_i(\cdot, 0), v_i(\cdot, 0) \in C([0, 1]), i = 1, 2$, s.t. (3.8)–(3.10) are satisfied at $t = 0$, and

$$\left. \begin{aligned} u_1(x, 0) + u_2(x, 0) &= 0, \\ v_1(x, 0) + v_2(x, 0) &= 0, \end{aligned} \right\} \forall x \in [0, 1]. \quad (4.2)$$

Then the solution $(u_i(x, t), v_i(x, t)), i = 1, 2$, satisfies

$$\left. \begin{aligned} u_1(x, t) + u_2(x, t) &= 0, \\ v_1(x, t) + v_2(x, t) &= 0, \end{aligned} \right\} \forall x \in [0, 1], \quad \forall t > 0. \quad (4.3)$$

Consequently, for any two solutions of (3.5) + (3.8)–(3.10) whose respective initial data satisfy (4.2), their linear superposition is again a solution (corresponding to the initial data that is the linear superposition of the two sets of given initial data).

Proof. The solution $u_i(x, t), v_i(x, t), i = 1, 2$, satisfies (3.13) and (3.14), whose RHS depend on the iterates of \mathcal{F}_I^k . Let

$$\begin{bmatrix} \bar{v}_1 \\ \bar{v}_2 \end{bmatrix} = \mathcal{F}_I^k \begin{bmatrix} \bar{u}_1 \\ \bar{u}_2 \end{bmatrix}, \quad \text{any } k = 1, 2, \dots,$$

where $\bar{u}_1 + \bar{u}_2 = 0$. But by Lemma 3.1, we see that

$$\begin{aligned} \bar{v}_1 + \bar{v}_2 &= \frac{1}{2}[(\bar{u}_1 - \bar{u}_2) + \tilde{F}^k(\bar{u}_1 + \bar{u}_2)] \\ &\quad + \frac{1}{2}[(-\bar{u}_1 + \bar{u}_2) + \tilde{F}^k(\bar{u}_1 + \bar{u}_2)] \\ &= \frac{1}{2}(\bar{u}_1 - \bar{u}_2) + \frac{1}{2}(-\bar{u}_1 + \bar{u}_2) \\ &= 0. \end{aligned} \quad (4.4)$$

We may take $\bar{u}_1 = u_1(x, 0)$ (resp., $v_1(x, 0)$) and $\bar{u}_2 = u_0(x, 0)$ (resp. $v_2(x, 0)$). By (4.2), (3.13) and (3.14), we conclude that (4.3) is satisfied, and the rule of linear superposition holds for all solutions with given initial data satisfying (4.2). ■

Similarly, we obtain the following.

Theorem 4.3 (*Linear Solutions for Two Nonlinearly Coupled Strings with a Type II Joint*). Con-

sider the PDE system (3.5), (3.8), (3.9) and (3.11), with $\alpha_{II} > 0$ and $\beta_{II} > 0$ in (3.11), and with given initial data $u_i(\cdot, 0), v_i(\cdot, 0) \in C([0, 1]), i = 1, 2$, s.t. (3.8), (3.9) and (3.11) are satisfied at $t = 0$, and

$$\left. \begin{aligned} u_1(x, 0) - u_2(x, 0) &= 0, \\ v_1(x, 0) - v_2(x, 0) &= 0, \end{aligned} \right\} \forall x \in [0, 1]. \quad (4.5)$$

Then the solution $(u_i(x, t), v_i(x, t)), i = 1, 2$, satisfies

$$\left. \begin{aligned} u_1(x, t) - u_2(x, t) &= 0, \\ v_1(x, t) - v_2(x, t) &= 0, \end{aligned} \right\} \forall x \in [0, 1], \quad t > 0, \quad (4.6)$$

Consequently, for any two solutions of (3.5) + (3.8) + (3.9) + (3.11) whose respective initial data satisfies (4.5), their linear superposition is again a solution (corresponding to the initial condition that is the linear superposition of the two sets of given initial data).

Example 4.1. Consider the original PDE system (2.17)–(2.20) and (2.22), where a Type I joint is placed at $x = 0$. Let the initial conditions be

$$\left. \begin{aligned} w_1(x, 0) \\ w_2(x, 0) \end{aligned} \right\} = \sum_{n=1}^{\infty} c_{1n} \sin n\pi x, \quad \begin{cases} -1 < x < 0, \\ 0 < x < 1, \end{cases} \quad (4.7)$$

and

$$\left. \begin{aligned} w_{1t}(x, 0) \\ w_{2,t}(x, 0) \end{aligned} \right\} = \sum_{n=1}^{\infty} n\pi c_{2n} \sin n\pi x, \quad \begin{cases} -1 < x < 0, \\ 0 < x < 1, \end{cases} \quad (4.8)$$

where the coefficients $\{c_{1n}, c_{2n}\}_{n=1}^{\infty}$ decay to zero sufficiently fast with respect to n . Then (2.24) is the solution of (2.17)–(2.20) + (2.22), which obeys the rule of linear superposition. By using (3.1)–(3.4), we get

$$\left. \begin{aligned} u_1(x, 0) &= -\frac{1}{2} \sum_{n=1}^{\infty} n\pi(c_{1n} + c_{2n}) \sin n\pi x, \\ u_2(x, 0) &= \frac{1}{2} \sum_{n=1}^{\infty} n\pi(c_{1n} + c_{2n}) \sin n\pi x, \\ v_1(x, 0) &= -\frac{1}{2} \sum_{n=1}^{\infty} n\pi(c_{1n} - c_{2n}) \sin n\pi x, \\ v_2(x, 0) &= \frac{1}{2} \sum_{n=1}^{\infty} n\pi(c_{1n} - c_{2n}) \sin n\pi x, \end{aligned} \right\} 0 < x < 1, \quad (4.9)$$

therefore (4.2) is satisfied, and Theorem 4.2 is applicable. This is consistent with the linearly superposed solution (2.24).

Example 4.2 (Nonlinear, Nonchaotic Vibrations which Eventually Become Linear Vibrations). We know from (3.33) (or, from [Chen *et al.*, 1995, Lemma 3.1]) that $0 = \tilde{F}(0)$, and 0 is a repelling fixed point of \tilde{F} . Let Ψ be the set of all preimages of 0 under \tilde{F} :

$$\Psi = \{u \in \mathbb{R} | \tilde{F}^k(u) = 0, \quad k = 1, 2, 3, \dots\}$$

$$= \bigcup_{k=1}^{\infty} \tilde{F}^{-k}(\{0\}).$$

It is clear from [Chen *et al.*, 1995, Sec. 4.1] that if

$$\alpha_i > 14, \quad \beta_i > 0, \quad i = I, II,$$

then Ψ is trivial: $\Psi = \{0\}$. But for

$$7.48878 \dots < \alpha_i \leq 14, \quad \beta_i > 0, \quad i = I, II,$$

we have $\Psi \supsetneq \{0\}$. Consider the line L in \mathbb{R}^2 :

$$L \equiv \{(u_1, u_2) \in \mathbb{R}^2 | u_1 + u_2 = 0\}.$$

It easily follows from Lemma 3.1 that

$$\mathcal{F}_I^{-k}(L) = \{(u_1, u_2) \in \mathbb{R}^2 | u_1 + u_2 \in \tilde{F}^{-k}(\{0\})\}.$$

Therefore, if the initial data $u_i(\cdot, 0), v_i(\cdot, 0) \in C([0, 1]), i = 1, 2$, in Theorem 4.2 do not satisfy (4.2), but instead, satisfy

$$\left. \begin{aligned} (u_1(x, 0), u_2(x, 0)) &\in \mathcal{F}_I^{-k}(L), \\ (v_1(x, 0), v_2(x, 0)) &\in \mathcal{F}_I^{-k}(L), \end{aligned} \right\} \quad \forall x \in [0, 1],$$

for some large positive integer k ,

then the solution of the PDE system (3.5) and (3.8)–(3.10) will not obey the rule of linear superposition (within this class of solutions). But the solution becomes linear vibrations after $t > 2k$, in the sense that (4.3) is satisfied for $t > 2k$ (instead of $t > 0$).

The final two theorems are the major results of this paper.

Theorem 4.4 (Linear Superposition of a Linear Solution and a Nonlinear Solution for Two Nonlinearly Coupled Strings with a Type I Joint). Let $(u_1(x, t), v_1(x, t), u_2(x, t), v_2(x, t))$ be the solution

of (3.5) and (3.8)–(3.10) with $\alpha_I > 0$ and $\beta_I > 0$ and with initial condition $(u_1(x, 0), v_1(x, 0), u_2(x, 0), v_2(x, 0))$ s.t. (4.2) and (4.3) are satisfied, and let $(U_1(x, t), V_1(x, t), U_2(x, t), V_2(x, t))$ be the solution of (3.5) and (3.8)–(3.10), with initial condition $(U_1(x, 0), V_1(x, 0), U_2(x, 0), V_2(x, 0))$ that does not satisfy (4.2) and (4.3). Then for any constant $C \in \mathbb{R}$,

$$(U_1(x, t) + Cu_1(x, t), V_1(x, t) + Cv_1(x, t), U_2(x, t) + Cu_2(x, t), V_2(x, t) + Cv_2(x, t))$$

is the solution to (3.5) and (3.8)–(3.10) corresponding to the initial condition

$$(U_1(x, 0) + Cu_1(x, 0), V_1(x, 0) + Cv_1(x, 0), U_2(x, 0) + Cu_2(x, 0), V_2(x, 0) + Cv_2(x, 0)).$$

Proof. It suffices to verify that $(U_1 + Cu_1, V_1 + Cv_1, U_2 + Cu_2, V_2 + Cv_2)$ satisfies (3.13) and (3.14). For any $x : 0 \leq x \leq 1, t = 2k + \tau, 0 \leq \tau < 2$, where k is an arbitrary nonnegative integer, consider for example, the case

$$x < \tau \leq 1 + x. \tag{4.10}$$

Then the middle equation in (3.13) is satisfied by U_i, V_i and $u_i, v_i, i = 1, 2$:

$$\begin{aligned} \begin{bmatrix} V_1(x, t) \\ V_2(x, t) \end{bmatrix} &= \mathcal{F}_I^{k+1} \left(\begin{bmatrix} U_1(\tau - x, 0) \\ U_2(\tau - x, 0) \end{bmatrix} \right), \\ \begin{bmatrix} v_1(x, t) \\ v_2(x, t) \end{bmatrix} &= \mathcal{F}_I^{k+1} \left(\begin{bmatrix} u_1(\tau - x, 0) \\ u_2(\tau - x, 0) \end{bmatrix} \right). \end{aligned}$$

Therefore

$$\begin{aligned} \begin{bmatrix} V_1(x, t) + Cv_1(x, t) \\ V_2(x, t) + Cv_2(x, t) \end{bmatrix} &= \mathcal{F}_I^{k+1} \left(\begin{bmatrix} U_1(\tau - x, 0) \\ U_2(\tau - x, 0) \end{bmatrix} \right) \\ &\quad + C \mathcal{F}_I^{k+1} \left(\begin{bmatrix} u_1(\tau - x, 0) \\ u_2(\tau - x, 0) \end{bmatrix} \right). \end{aligned} \tag{4.11}$$

But, since $u_i, v_i, i = 1, 2$, satisfy (4.2) and (4.3), by Lemma 3.1, we have

$$\begin{aligned} &\mathcal{F}_I^{k+1} \left(\begin{bmatrix} u_1(\tau - x, 0) \\ u_2(\tau - x, 0) \end{bmatrix} \right) \\ &= \begin{bmatrix} \frac{1}{2}(u_1(\tau - x, 0) - u_2(\tau - x, 0)) \\ \frac{1}{2}(-u_1(\tau - x, 0) + u_2(\tau - x, 0)) \end{bmatrix}. \end{aligned} \tag{4.12}$$

On the other hand, by Lemma 3.1,

$$\mathcal{F}_I^{k+1} \left(\begin{bmatrix} U_1(\tau-x, 0) \\ U_2(\tau-x, 0) \end{bmatrix} \right) = \frac{1}{2} \left[\begin{aligned} & (U_1(\tau-x, 0) - U_2(\tau-x, 0)) + \tilde{F}^{k+1}(U_1(\tau-x, 0) + U_2(\tau-x, 0)) \\ & (-U_1(\tau-x, 0) + U_2(\tau-x, 0)) + \tilde{F}^{k+1}(U_1(\tau-x, 0) + U_2(\tau-x, 0)) \end{aligned} \right]. \tag{4.13}$$

By (4.11)–(4.13) and (4.2), we therefore get

$$\begin{bmatrix} V_1(x, t) + Cv_1(x, t) \\ V_2(x, t) + Cv_2(x, t) \end{bmatrix} = \frac{1}{2} \left[\begin{aligned} & ([U_1(\tau-x, 0) + Cu_1(\tau-x, 0)] - [U_2(\tau-x, 0) + Cu_2(\tau-x, 0)]) \\ & + \tilde{F}^{k+1}([U_1(\tau-x, 0) + Cu_1(\tau-x, 0)] + [U_2(\tau-x, 0) + Cu_2(\tau-x, 0)]) \\ & (-[U_1(\tau-x, 0) + Cu_1(\tau-x, 0)] + [U_2(\tau-x, 0) + Cu_2(\tau-x, 0)]) \\ & + \tilde{F}^{k+1}([U_1(\tau-x, 0) + Cu_1(\tau-x, 0)] + [U_2(\tau-x, 0) + Cu_2(\tau-x, 0)]) \end{aligned} \right].$$

Hence $U_i + Cu_i, V_i + Cv_i, i = 1, 2$, also satisfy the middle equation of (3.13) in the case of (4.10). The other cases in (3.13) and (3.14) can be verified similarly. Therefore $(U_i + Cu_i, V_i + Cv_i), i = 1, 2$, is the solution to (3.5) and (3.8)–(3.12) with initial data $(U_i(x, 0) + Cu_i(x, 0), V_i(x, 0) + Cv_i(x, 0)), i = 1, 2$. ■

Similarly, we conclude the following.

Theorem 4.5 (*Linear Superposition of a Linear Solution and a Nonlinear Solution for Two Nonlinearly Coupled Strings with a Type II Joint*). Let $(u_1(x, t), v_1(x, t), u_2(x, t), v_2(x, t))$ be the solution of (3.5), (3.8), (3.9) and (3.11) with $\alpha_{II} > 0$ and $\beta_{II} > 0$ and with initial condition $(u_1(x, 0), v_1(x, 0), u_2(x, 0), v_2(x, 0))$ s.t. (4.5) and (4.6) are satisfied, and let $(U_1(x, t), V_1(x, t), U_2(x, t), V_2(x, t))$ be the solution of (3.5), (3.8), (3.9) and (3.11), with initial condition $(U_1(x, 0), V_1(x, 0), U_2(x, 0), V_2(x, 0))$ that do not satisfy (4.5) and (4.6). Then for any constant $C \in \mathbb{R}$,

$$\begin{aligned} & (U_1(x, t) + Cu_1(x, t), V_1(x, t) + Cv_1(x, t), \\ & U_2(x, t) + Cu_2(x, t), V_2(x, t) + Cv_2(x, t)) \end{aligned}$$

is the solution to (3.5), (3.8), (3.9) and (3.11) corresponding to the initial condition

$$\begin{aligned} & (U_1(x, 0) + Cu_1(x, 0), V_1(x, 0) + Cv_1(x, 0), \\ & U_2(x, 0) + Cu_2(x, 0), V_2(x, 0) + Cv_2(x, 0)). \end{aligned}$$

5. Numerical Simulations and Graphics

We include some numerical examples in this section to show that linear and chaotic vibrations can co-exist, and satisfy the rule of linear superposition. Throughout this section, we consider only a Type I

joint. The parameters are chosen to be $\alpha_I = 8.5$ and $\beta_I = 8$ in the range (4.1). By Theorem 4.1, the mapping \mathcal{F}_I is chaotic.

Example 5.1 (Linear Periodic Vibrations). For the PDE system (3.5) and (3.8)–(3.10), choose the initial data

$$\left. \begin{aligned} u_1(x, 0) &= -\sin 2\pi x, \\ v_1(x, 0) &= \sin 2\pi x, \\ u_2(x, 0) &= \sin 2\pi x, \\ v_2(x, 0) &= -\sin 2\pi x, \end{aligned} \right\} 0 \leq x \leq 1. \tag{5.1}$$

Then (4.2) is satisfied, and Theorem 4.2 is applicable.

The solution $u_i(x, t), v_i(x, t), i = 1, 2$, is solved by using formulas (3.13) and (3.14). Because $u_1(x, t)$ and $v_1(x, t)$ were defined from w_1 through (3.1) and (3.2) while $w_1(x, t)$ is defined for $-1 \leq x \leq 0$, let us reintroduce notation

$$\left. \begin{aligned} \bar{u}_1(x, t) &= -v_1(-x, t), \\ \bar{v}_1(x, t) &= -u_1(-x, t), \end{aligned} \right\} -1 \leq x \leq 0, \quad t \geq 0, \\ \left. \begin{aligned} \bar{u}_2(x, t) &= u_2(x, t), \\ \bar{v}_2(x, t) &= v_2(x, t), \end{aligned} \right\} 0 \leq x \leq 1, \quad t \geq 0, \tag{5.2}$$

so that $\bar{u}_i, \bar{v}_i, i = 1, 2$, can be displayed on the natural spatial interval $[-1, 0] \cup [0, 1] \ni x$. According to the change of variables (5.2), the initial condition (5.1) is plotted as the solid curve in Fig. 4. The solution (5.2) is plotted in Figs. 5–8 for time durations [10, 12] and [50, 52]. The periodic nature of the solution can be easily seen from these figures.

Example 5.2 (Superposition of Linear and Chaotic Vibrations). Suppose $U_i(x, t), V_i(x, t), i = 1, 2$, is a solution of (3.5) and (3.8)–(3.10) with initial data $U_i(x, 0), V_i(x, 0), i = 1, 2$, which is genuinely

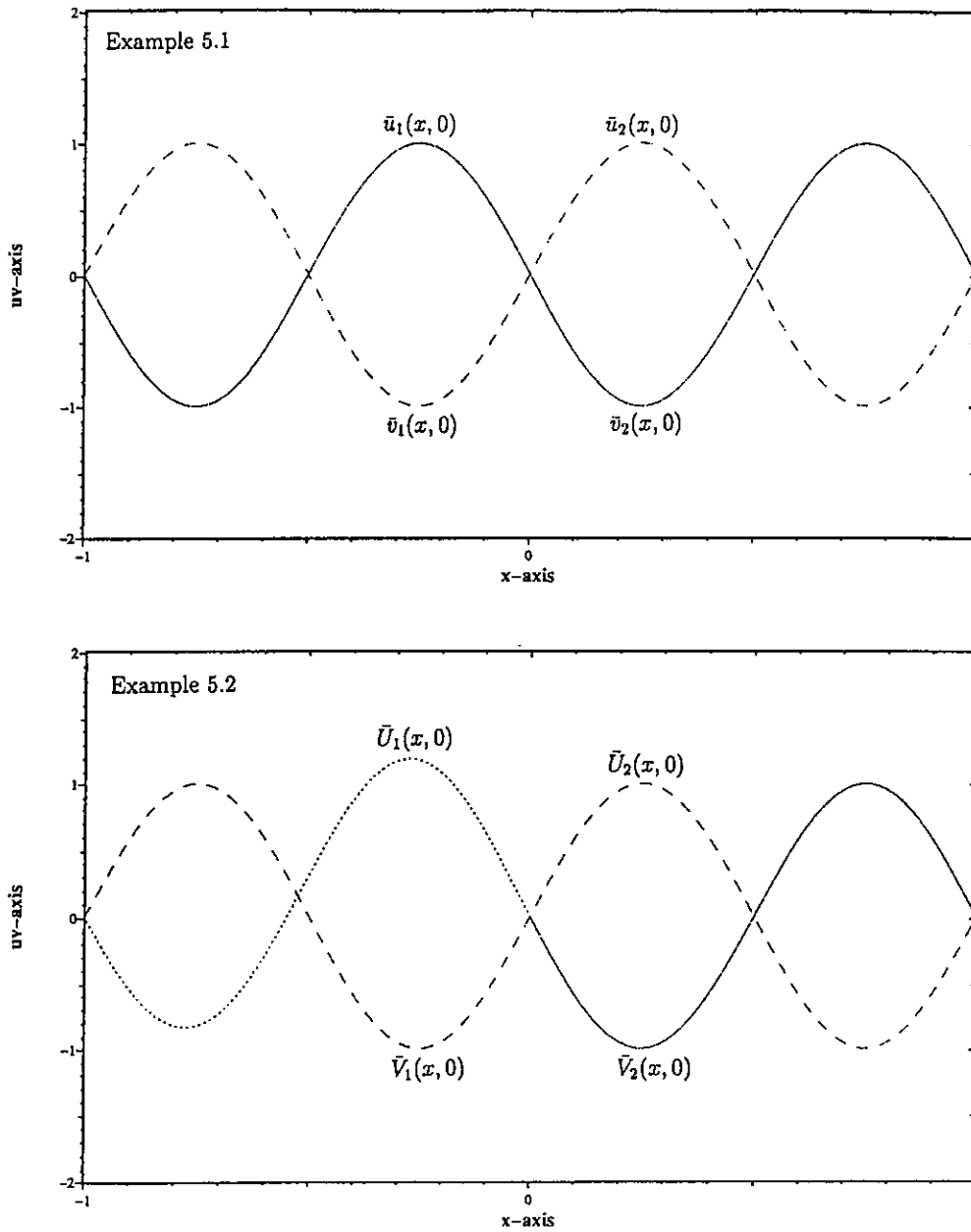


Fig. 4. The initial data of Examples 5.1 and 5.2, plotted on $[-1, 1]$ according to change of variables formula (5.2).

nonlinear in the sense that (4.3) and (4.4) are not satisfied.

Even though \mathcal{F}_I is a chaotic interval map, the solution $U_i, V_i, i = 1, 2$, satisfying (3.13) and (3.14) may not manifest chaotic dynamic behavior because if

$$\begin{aligned} J_1 &\equiv \text{supp}[U_1(x, 0) + U_2(x, 0)], \\ J_2 &\equiv \text{supp}[V_1(x, 0) + V_2(x, 0)] \quad (5.3) \\ (\text{supp} &\equiv \text{support of a given function}) \end{aligned}$$

contain only periodic (or eventually periodic) points

of \tilde{F} , then by Lemma 3.1 and (3.13) and (3.14), we easily see that $U_i(x, t), V_i(x, t), i = 1, 2$, will not manifest dynamic chaotic behavior. In order for $U_i(x, t)$ and $V_i(x, t), i = 1, 2$, to contain chaos, the intervals J_1 and J_2 in (5.2) and (5.3) must be sufficiently large s.t. (3.6) holds for \tilde{F} , i.e.,

$$\left. \begin{aligned} \text{range}_{x \in \tilde{J}_1} \rho_A(x) &\supseteq (\delta_1, \delta_2), \text{ or } \text{range}_{x \in \tilde{J}_2} \rho_A(x) \supseteq (\delta_1, \delta_2), \\ \text{for some } 0 < \delta_1 < \delta_2, &\text{ for some closed interval } A, \end{aligned} \right\} \quad (5.4)$$

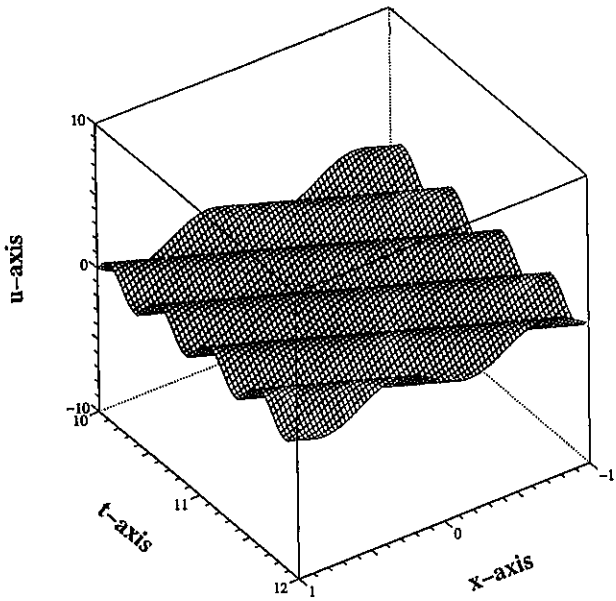


Fig. 5. The linear solution $\bar{u}_1(x, t)$ and $\bar{u}_2(x, t)$ on the spatial span $[-1, 1] \ni x$, for the time duration $[10, 12] \ni t$, of Example 5.1. (The part $\bar{u}_1(x, t)$ lives on the spatial interval $x \in [-1, 0]$, while the part $\bar{u}_2(x, t)$ lives on $x \in [0, 1]$.) This linear solution is periodic.

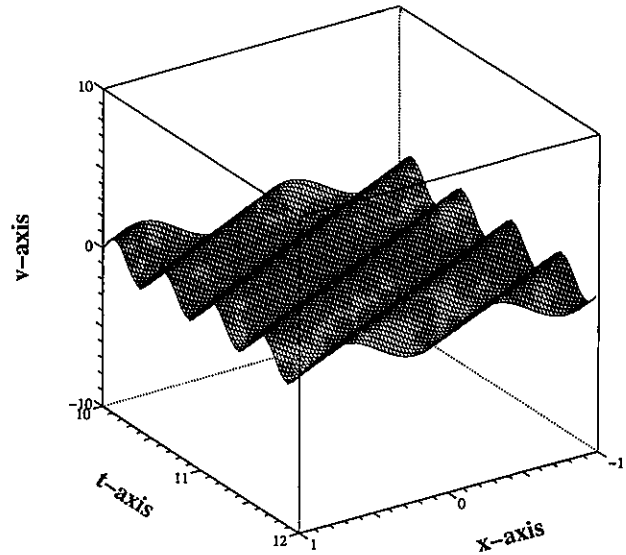


Fig. 7. The linear solution $\bar{v}_1(x, t)$ and $\bar{v}_2(x, t)$ on the spatial span $[-1, 1] \ni x$, for the time duration $[10, 12] \ni t$, of Example 5.1. Again note the periodicity of the solution.

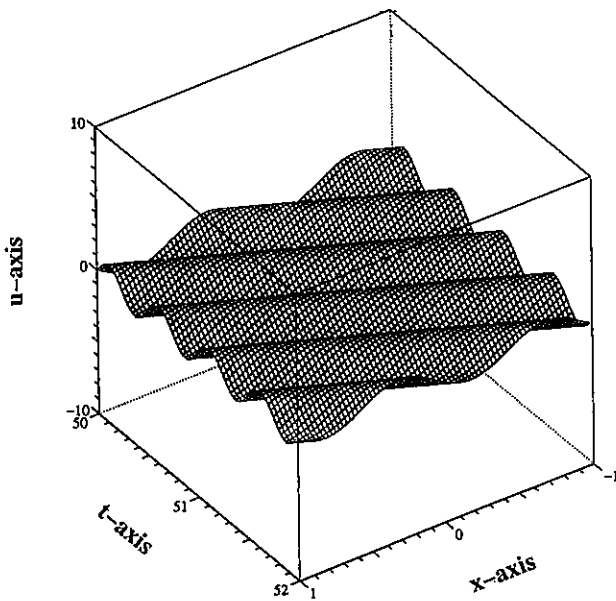


Fig. 6. The linear solution $\bar{u}_1(x, t)$ and $\bar{u}_2(x, t)$ on the spatial span $[-1, 1] \ni x$, for the time duration $[50, 52] \ni t$, of Example 5.1. The solution profile is identical to that in Fig. 5 because the solution is periodic with period 1.

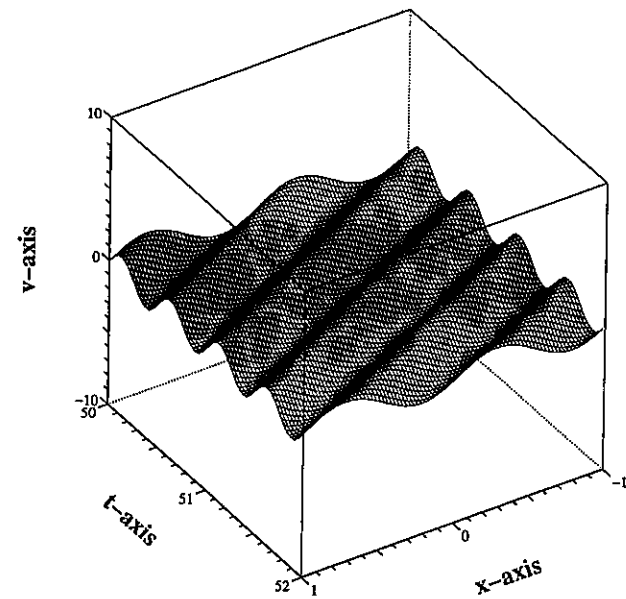


Fig. 8. The linear solution $\bar{v}_1(x, t)$ and $\bar{v}_2(x, t)$ on the spatial span $[-1, 1] \ni x$, for the time duration $[50, 52] \ni t$, of Example 5.1. This profile is identical to that of Fig. 7.

where

$$\begin{aligned} \tilde{J}_1 &= \tilde{F}^\ell(J_1) \subseteq I, \quad \tilde{J}_2 = \tilde{F}^\ell(J_2) \subseteq I; \\ I &\text{ is a nontrivial interval s.t.} \\ \tilde{F} &: I \rightarrow I, \quad \text{and } A \subseteq I, \end{aligned} \tag{5.5}$$

for some positive integer ℓ sufficiently large. (The existence of such an ℓ is clear because $I \times I$ is a global invariant rectangle.)

Let us choose the initial data to be

$$\left. \begin{aligned} U_1(x, 0) &= -\sin 2\pi x + 5x^2(1-x)^2, \\ V_1(x, 0) &= -\sin 2\pi x, \\ U_2(x, 0) &= \sin 2\pi x, \\ V_2(x, 0) &= -\sin 2\pi x, \end{aligned} \right\} 0 \leq x \leq 1. \tag{5.6}$$

Then

$$J_1 = \left[0, \max_{0 \leq x \leq 1} 5x^2(1-x)^2\right] = \left[0, \frac{5}{16}\right] \tag{5.7}$$

$$J_2 = \{0\}. \tag{5.8}$$

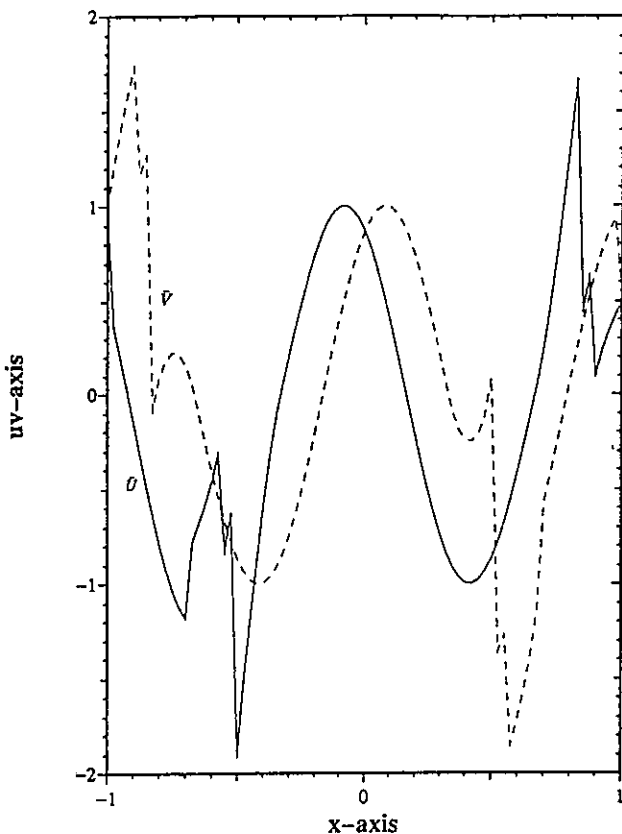


Fig. 9. The solution $\bar{U}_i(x, t), \bar{V}_i(x, t), i = 1, 2$, on the spatial span $[-1, 1] \ni x$, at time $t = 11\frac{1}{3}$, of Example 5.2. These are nonlinear solutions. Irregular vibration patterns begin to appear.

The global invariant rectangle $I \times I$ is found with

$$\begin{aligned} I &= \left[- \left(\sqrt{\frac{(\alpha_I/2)-1}{3 \cdot (\beta_I/8)}} + \frac{(\alpha_I/2)-1}{3} \sqrt{\frac{(\alpha_I/2)-1}{3(\beta_I/8)}} \right), \right. \\ &\quad \left. \sqrt{\frac{(\alpha_I/2)-1}{3 \cdot (\beta_I/8)}} + \frac{(\alpha_I/2)-1}{3} \sqrt{\frac{(\alpha_I/2)-1}{3(\beta_I/8)}} \right] \\ &= \left[- \left(\sqrt{\frac{4.25-1}{3}} + \frac{(4.25-1)}{3} \sqrt{\frac{4.25-1}{3}} \right), \right. \\ &\quad \left. \sqrt{\frac{4.25-1}{3}} + \frac{(4.25-1)}{3} \sqrt{\frac{4.25-1}{3}} \right] \\ &\approx [-2.1684, 2.1684]; \end{aligned} \tag{5.9}$$

cf. [Chen *et al.*, 1995, Case (4.3.i)]. We did not rigorously verify (5.4) for (5.7)–(5.9), but based upon

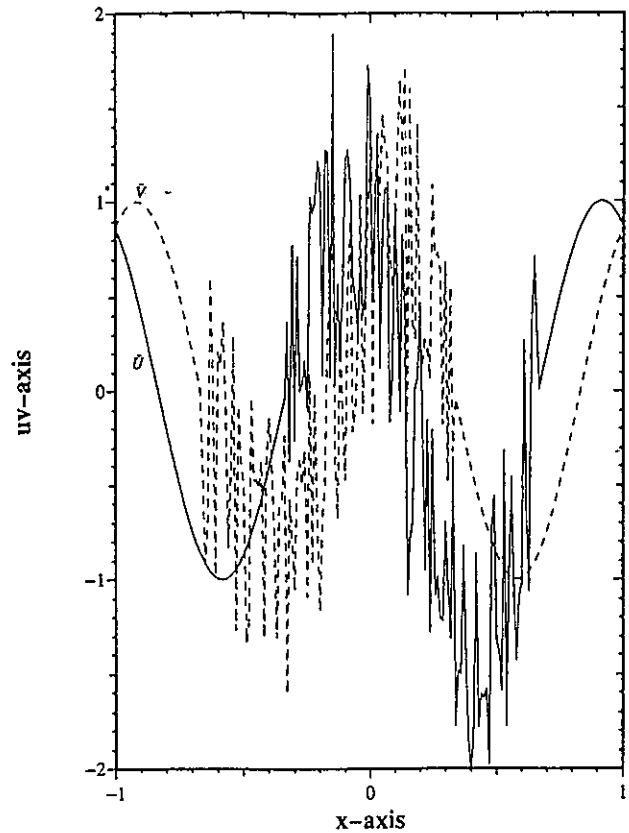


Fig. 10. The solution $\bar{U}_i(x, t), \bar{V}_i(x, t), i = 1, 2$, on the spatial span $[-1, 1] \ni x$, at time $t = 50\frac{1}{3}$, of Example 5.2. As time becomes progressively large, disorderly vibrations become prominent. Note that \bar{U} and \bar{V} are actually quite smooth on half of the spatial span $[-1, 1]$. This is due to the fact that chaotic disturbances propagate with a unit speed and are nondispersive; they exist only on half of the spatial span $[-1, 1]$ at any time.

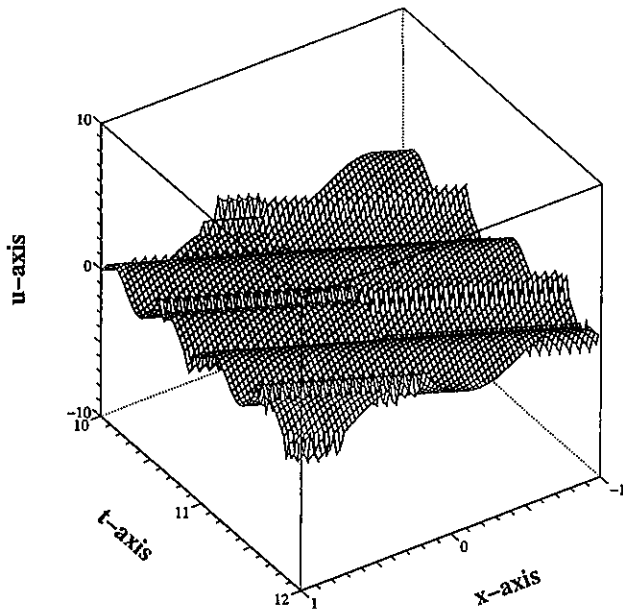


Fig. 11. The solution $\bar{U}_1(x, t)$ and $\bar{U}_2(x, t)$ on the spatial spans $[-1, 1] \ni x$, for the time duration $[10, 12] \ni t$, of Example 5.2. Chaotic vibrations are seen to be “piggybacking” on linear periodic vibrations.

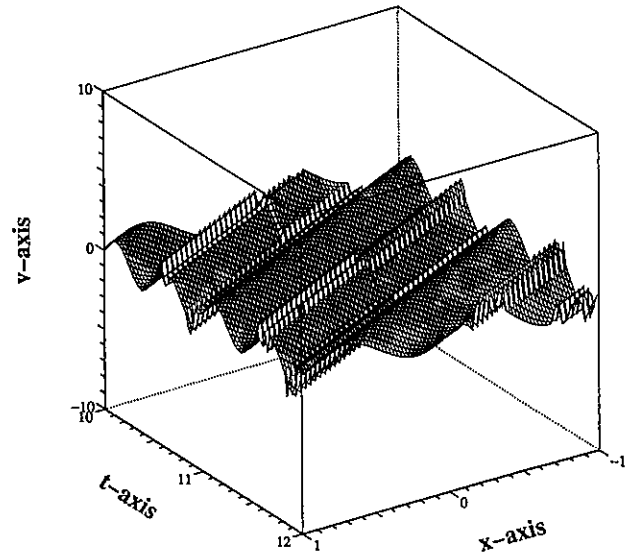


Fig. 13. The solution $\bar{V}_1(x, t)$ and $\bar{V}_2(x, t)$ on the spatial span $[-1, 1] \ni x$, for the time duration $[10, 12] \ni t$, of Example 5.2.

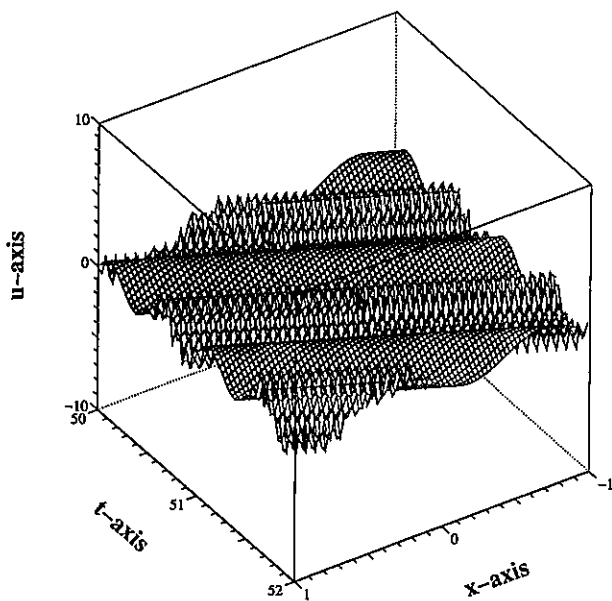


Fig. 12. The solution $\bar{U}_1(x, t)$ and $\bar{U}_2(x, t)$ on the spatial span $[-1, 1] \ni x$, for the time duration $[50, 52] \ni t$, of Example 5.2. In comparison with Fig. 11, the magnitude of chaotic vibrations become more prominent.

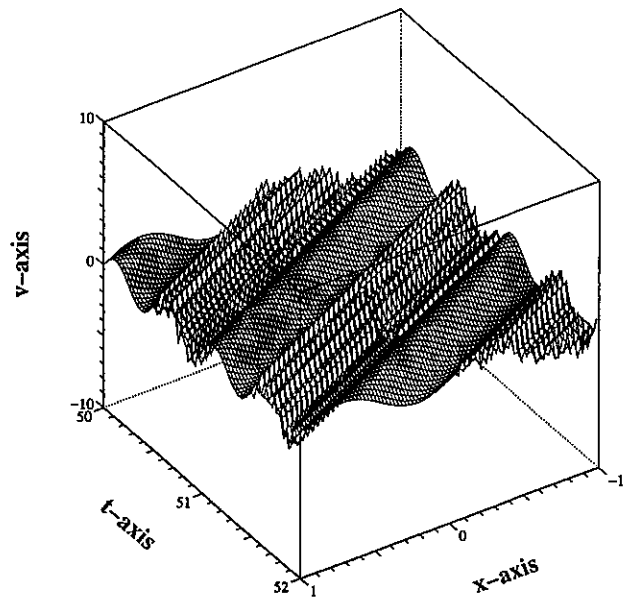


Fig. 14. The solution $\bar{V}_1(x, t)$ and $\bar{V}_2(x, t)$ on the spatial span $[-1, 1] \ni x$, for the time duration $[50, 52] \ni t$, of Example 5.2. In comparison with Fig. 13, we again observe the coexistence of linear and chaotic vibrations, and that the magnitude of chaotic vibrations has increased.

our knowledge in [Chen *et al.*, 1995], we know that (5.4) is true.

Note that the $\pm \sin 2\pi x$ terms in the initial data (5.6) will generate the linear periodic solution in Example 5.1. The term $5x^2(1-x)^2$ in (5.6) will cause chaotic dynamic behavior of U_i and V_i , $i = 1, 2$. We solve U_i, V_i , $i = 1, 2$, according to (3.13) and (3.14). The graphs of \bar{U}_i, \bar{V}_i , $i = 1, 2$, cf. (5.2), are plotted for $t = 11\frac{1}{3}, 50\frac{1}{3}$, and for the time durations [10, 12] and [50, 52]; see Figs. 9–14. The reader can easily observe that chaotic vibrations are “piggy-backing” on the linear periodic vibrations (waves) in Figs. 5–8 of Example 5.1.

Another interesting phenomenon may also be observed. In (5.6), the perturbation term $5x^2(1-x)^2$ causing chaos lives only on half of the natural spatial span $[-1, 0] \cup [0, 1]$ of the coupled string system. From Figs. 9 and 10, we see that chaotic vibrations are happening on only half length of the total span $[-1, 0] \cup [0, 1]$. This is due to the single speed nondispersive wave propagation on the coupled string system.

Acknowledgments

G. Chen and J. Zhou were partially supported by NSF Grant DMS 9404380, Texas A&M University Interdisciplinary Research Initiative IRI 96-39, and Texas ARP Grant 010366-046. S. B. Hsu was partially supported by Grant NSC 83-0208-M-007-071 from the National Council of Science of Republic of China.

References

- Chen, G. & Zhou, J. [1993] *Vibration and Damping in Distributed Systems, Vol. I: Analysis, Estimation, Attenuation and Design* (CRC Press, Boca Raton, FL).
- Chen, G., Hsu, S. B. & Zhou, J. [1995] “Chaotic vibrations of the infinite dimensional harmonic oscillator due to a self-excitation boundary condition, Part I: Controlled hysteresis,” preprint.
- Chen, G. R. & Dong, X. [1993] “From chaos to order—perspectives and methodologies in controlling chaotic nonlinear dynamical systems,” *Int. J. Bifurcation and Chaos* **3**(6), 1363–1409.
- Devaney, R. L. [1989] *An Introduction to Chaotic Dynamical Systems* (Addison-Wesley, New York).
- Guckenheimer, J. & Holmes, P. [1983] *Nonlinear Oscillations, Dynamical Systems, and Bifurcation of Vector Fields* (Springer-Verlag, New York).
- Keener, J. P. [1980] “Chaotic behavior in piecewise continuous difference equations,” *Trans. Amer. Math. Soc.* **261**, 589–604.
- Lagnese, J. E., Leuguring, G. & Schmidt, G. [1994] *Modeling, Analysis and Control of Multi-Link Flexible Structures* (Birkhauser, Boston).
- Moon, F. C. [1987] *Chaotic Vibrations* (Wiley-Interscience, New York).
- SIAM [1995] *Final Program and Abstracts of the Third SIAM Conference on Applications of Dynamical Systems*, May, 1995, Snowbird, Utah, published by SIAM, Philadelphia, May, 1995.
- Stoker, J. J. [1950] *Nonlinear Vibrations* (Wiley-Interscience, New York).
- Wiggins, S. [1990] *Introduction to Applied Nonlinear Dynamical Systems and Chaos* (Springer-Verlag, New York).